

N-particle irreducible actions for stochastic fluids

Jingyi Chao^a Thomas Schäfer^b

^a*College of Physics and Communication Electronics, Jiangxi Normal University, Nanchang 330022, China*

^b*Department of Physics, North Carolina State University, Raleigh, NC 27695*

E-mail: chaojingyi@jxnu.edu.cn, tmschaef@ncsu.edu

ABSTRACT: We construct one- and two-particle irreducible (1PI and 2PI) effective actions for the stochastic fluid dynamics of a conserved density undergoing diffusive motion. We compute the 1PI action in one-loop order and the 2PI action in two-loop approximation. We derive a set of Schwinger-Dyson equations and regularize the resulting equations using Pauli-Villars fields. We numerically solve the Schwinger-Dyson equations for a non-critical fluid. We find that higher-loop effects summed by the Schwinger-Dyson renormalize the non-linear coupling. We also find indications of a diffuson-cascade, the appearance of n -loop correction with smaller and smaller exponential suppression.

ARXIV EPRINT: [2302.00720](https://arxiv.org/abs/2302.00720)

Contents

1	Introduction	1
2	1PI effective action	2
3	2PI effective action	5
4	Gap equation in mixed representation	8
5	Conclusions and Outlook	10
A	Pauli-Villars Regulator	12

1 Introduction

The study of hydrodynamic fluctuations has received renewed interest in connection with the experimental search for a conjectured critical endpoint in the phase diagram of Quantum Chromodynamics (QCD) [1–4]. The basic idea is that the quark-gluon plasma created in a heavy ion collision is a locally equilibrated fluid, and that each fluid element traces out a trajectory in the QCD phase diagram. If the trajectory approaches a critical point then the correlation length will grow, and fluctuations of thermodynamic variables are enhanced. At freezeout fluctuations in the fluid are converted to fluctuations of particle distributions, which can be measured experimentally. A typical set of observables is given by the cumulants of the net-proton number in a given rapidity window.

In thermodynamic equilibrium fluctuations in conserved densities are governed by susceptibilities, which can be obtained as derivatives of the thermodynamic potential. The theory of second-order phase transitions predicts that near the critical point susceptibilities scale as powers of the correlation length ξ , where higher-order susceptibilities scale with a larger power of ξ . Higher-order susceptibilities also potentially exhibit an oscillatory dependence on control parameters, such as the temperature and the baryon chemical potential. Both of these observations imply that non-Gaussian cumulants provide crucially consistency checks for the possible discovery of a critical endpoint [5–9].

The fluid created in a heavy ion collision expands rapidly, and fluctuation observables are expected to deviate from equilibrium expectations. In the vicinity of a critical point non-equilibrium phenomena, such as critical slowing down cannot be ignored [3, 4, 10–12]. Dynamical critical scaling predicts the dependence of the relaxation time τ on the correlation length, $\tau \sim \xi^z$, where z is the dynamical critical exponent [13]. While the value of z for theories in a different universality classes are known from numerical calculations and the epsilon expansion [13, 14], less is known about the functional form of time-dependent n -point functions, and the relative relaxation rate of n -point functions for different n .

Several methods for studying hydrodynamic n -point functions have been explored in the literature. This includes numerical simulations of stochastic fluid dynamics [11, 15–20], dynamical evolution equations for n -point functions [12, 21–27], as well as hydrodynamic effective actions [28–31]. In previous work we considered a pure perturbative approach to effective actions for fluid dynamics [30]. In the present paper we study a non-perturbative approach based on n -particle irreducible effective actions, see [32, 33] for a review. In the following we develop the formalism in the context of a simple model of non-linear diffusion, and we study a numerical solution of the Schwinger-Dyson equation for the two-point function in a non-critical theory.

2 1PI effective action

We consider a conserved density $\psi(x, t)$. In thermal equilibrium the probability distribution of ψ is governed by a free energy functional

$$\mathcal{F}[\psi] = \int d^3x \left\{ \frac{1}{2} (\vec{\nabla}\psi)^2 + \frac{m^2}{2} \psi(x, t)^2 + \frac{\lambda_3}{3!} \psi(x, t)^3 + \dots \right\}. \quad (2.1)$$

where \dots contains higher-order non-linearities. Of course, for the theory to be stable there has to be a fourth-order (or higher order even) interaction present as well. In the vicinity of a critical point in the Ising universality class there is an emergent Z_2 symmetry and the cubic term is absent, but at a generic point in the phase diagram a cubic non-linearity is present. The dynamics of the theory are governed by a diffusion equation

$$\partial_t \psi(x, t) = \kappa \nabla^2 \left(\frac{\delta \mathcal{F}[\psi]}{\delta \psi(x, t)} \right) + \theta(x, t), \quad (2.2)$$

where κ is a conductivity, $D = \kappa m^2$ is the diffusion constant, and $\theta(x, t)$ is a noise term. The noise has zero mean $\langle \theta(x, t) \rangle = 0$ and correlation

$$\langle \theta(x, t) \theta(x', t') \rangle = -\kappa T \nabla^2 \delta(x - x') \delta(t - t'). \quad (2.3)$$

The structure of the noise correlator is fixed by fluctuation-dissipation relations, and ensures that the equilibrium distribution is given by $P[\psi] \sim \exp(-\mathcal{F}[\psi]/T)$.

The observables of the theory are correlation functions of the density $\psi(x, t)$ averaged over different realizations of the noise. It is well known that these correlation functions can be derived from an effective lagrangian that contains an additional auxiliary field $\tilde{\psi}$ [28, 29, 34–36]. The effective lagrangian is given by

$$\mathcal{L} = \tilde{\psi} (\partial_t - D \nabla^2) \psi + \kappa T \tilde{\psi} \nabla^2 \tilde{\psi} - \frac{\kappa \lambda_3}{2} \tilde{\psi} \nabla^2 \psi^2 + \dots \quad (2.4)$$

Note that the variation of the action with respect to $\tilde{\psi}$ leads to a stochastic diffusion equation for ψ , where the structure of the noise term is governed by the quadratic term in $\tilde{\psi}$. We consider the partition function

$$Z[J, \tilde{J}] = \int D\psi D\tilde{\psi} \exp(-S), \quad S = \int dt d^3x \left\{ \mathcal{L} + \tilde{J}\tilde{\psi} + J\psi \right\}. \quad (2.5)$$

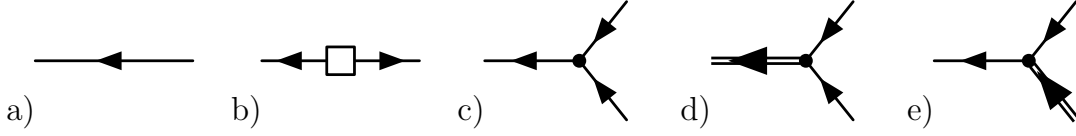


Figure 1. Feynman rules for the calculation of the 1PI effective action. Fig. a) shows the propagator $\langle \delta\psi\delta\tilde{\psi} \rangle$, b) is the propagator $\langle \delta\psi\delta\psi \rangle$, c) is the non-linear $\delta\tilde{\psi}(\delta\psi)^2$ interaction, and d,e) are the coupling to the classical fields $\tilde{\Psi}$ and Ψ , respectively.

We define $\exp(-W) = Z$. Then

$$\frac{\delta W}{\delta J} = \langle \psi \rangle = \Psi, \quad \frac{\delta W}{\delta \tilde{J}} = \langle \tilde{\psi} \rangle = \tilde{\Psi}, \quad (2.6)$$

and we can define the Legendre transform

$$\Gamma[\Psi, \tilde{\Psi}] = W[J, \tilde{J}] - \int dt d^3x \left(J\Psi + \tilde{J}\tilde{\Psi} \right). \quad (2.7)$$

This relation defined the 1PI effective action Γ . We can compute the effective action using the background field method. We write

$$\psi = \Psi + \delta\psi, \quad \tilde{\psi} = \tilde{\Psi} + \delta\tilde{\psi}. \quad (2.8)$$

Then

$$S[\psi, \tilde{\psi}] = S[\Psi, \tilde{\Psi}] + \int dt d^3x \left(\frac{\delta S}{\delta \Psi} \delta\psi + \frac{\delta S}{\delta \tilde{\Psi}} \delta\tilde{\psi} \right) + S_2[\delta\psi, \delta\tilde{\psi}, \Psi, \tilde{\Psi}], \quad (2.9)$$

where the fluctuation term S_2 is given by

$$S_2[\delta\psi, \delta\tilde{\psi}, \Psi, \tilde{\Psi}] = \int dt d^3x \left\{ \delta\tilde{\psi} (\partial_t - D\nabla^2) \delta\psi + \kappa T \delta\tilde{\psi} \nabla^2 \delta\tilde{\psi} - \frac{\kappa\lambda_3}{2} \delta\tilde{\psi} \nabla^2 (\delta\psi)^2 - \frac{\kappa\lambda_3}{2} \left[(\nabla^2 \tilde{\Psi})(\delta\psi)^2 + 2(\nabla^2 \delta\tilde{\psi})(\delta\psi)\Psi \right] \right\}. \quad (2.10)$$

We can now perform the Legendre transform. We find

$$\Gamma[\Psi, \tilde{\Psi}] = S[\Psi, \tilde{\Psi}] + \Gamma_F[\Psi, \tilde{\Psi}], \quad (2.11)$$

where Γ_F , the fluctuation term, is

$$\Gamma_F[\Psi, \tilde{\Psi}] = \int D(\delta\psi\delta\tilde{\psi}) \exp \left(-S_2[\delta\psi, \delta\tilde{\psi}, \Psi, \tilde{\Psi}] \right). \quad (2.12)$$

The 1PI effective action is given by the classical action $S[\Psi, \tilde{\Psi}]$ and fluctuation corrections generated by S_2 . These corrections can be computed perturbatively, using the Feynman rules shown in Fig. 1. The Feynman rules for the fluctuating fields are identical to those given in our earlier work, see equ. (3.1-3.3) in [30]. The vertices for Ψ and $\tilde{\Psi}$ are new, and follow by substitution from the cubic vertex $\tilde{\psi}\nabla^2(\psi^2)$.

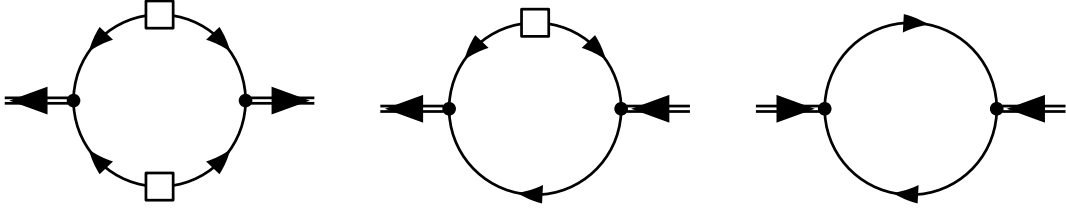


Figure 2. One-loop contributions to the 1PI effective action. The left panel shows the $\tilde{\Psi}^2$ term in equ. (2.13), and the middle panel is the $\tilde{\Psi}\Psi$ term. The right panel shows the Ψ^2 term, which vanishes.

We expand Γ_F in powers of Ψ and $\tilde{\Psi}$. Linear terms correspond to tadpole diagrams, which vanish. One-loop contributions to the quadratic terms are shown in Fig. 2. Higher loop corrections are suppressed by powers of the external momentum. The one-loop terms are

$$\Gamma_F[\Psi, \tilde{\Psi}] = \int dt dt' d^3x d^3x' \tilde{\Psi}(x, t) \Psi(x', t') \Sigma(x - x', t - t') + \int dt dt' d^3x d^3x' \tilde{\Psi}(x, t) \tilde{\Psi}(x', t') \delta D(x - x', t - t'). \quad (2.13)$$

In a large homogeneous system the self energies Σ and δD can be computed in frequency-momentum (ω, k) space. Using the results from [29, 30] we have

$$\Sigma(\omega, k) = \frac{i\lambda_3^2 T}{32\pi m^6} \omega k^2 \sqrt{k^2 - \frac{2i\omega}{D}}, \quad (2.14)$$

$$\delta D(\omega, k) = \frac{D\lambda_3^2 T^2}{16\pi m^8} k^4 \text{Re} \sqrt{k^2 - \frac{2i\omega}{D}}. \quad (2.15)$$

We can now determine equations of motion for $(\Psi, \tilde{\Psi})$ that include the fluctuation effects encoded in equ. (2.14, 2.15). In particular, there is a "classical solution" with $\tilde{\Psi} = 0$ and

$$(\partial_t - D\nabla^2)\Psi - \frac{\kappa\lambda_3^2}{2} \nabla^2 \Psi^2 + \int d^3x' dt' \Psi(x', t') \Sigma(x, t; x', t') = 0. \quad (2.16)$$

Here, the first term is the classical diffusion equation, the second term encodes nonlinearities, and the third term accounts for fluctuation effects. To understand these effects, consider a mixed representation $\Psi_k(t)$, where we have performed a Fourier transform with respect to the spatial coordinate. The classical diffusion equation corresponds to an exponential decay, $\Psi_k(t) \sim \exp(-Dk^2 t) \Psi_k(0)$. Fluctuation effects are described by the mixed-representation self energy $\Sigma(t, k)$. Using the one-loop result in equ. (2.14) we get

$$\Sigma(t, k) = \frac{3(\kappa\lambda_3)^2}{16\pi^{3/2}} \frac{Tk^2}{m^2} \Theta(t) \exp\left(-\frac{Dk^2 t}{2}\right) \left\{ \frac{1}{(2Dt)^{5/2}} + \frac{k^2}{6(2Dt)^{3/2}} \right\}, \quad (2.17)$$

where we have performed the Fourier transform using contour integration. The fractional powers of t characterize a long time tails in the evolution of the density due to fluctuations.

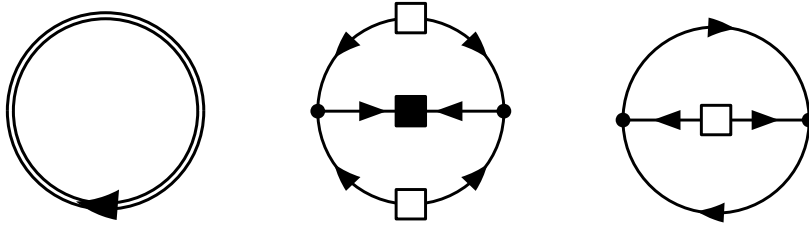


Figure 3. One and two-loop contributions to the 2PI effective action. Here, the left panel corresponds to $\text{Tr} \log G$, and the middle and the right panel are two-loop diagrams constructed from the vertex in S_3 and the propagators G_{12} , G_{21} (solid lines), G_{22} (line with open box), and G_{11} (line with solid box).

The correction to the noise term is given by

$$\delta D(t, k) = \frac{(\kappa \lambda_3)^2}{32\pi^{3/2}} \frac{T^2}{m^4} \frac{k^4}{(2D|t|)^{3/2}} \exp\left(-\frac{Dk^2|t|}{2}\right). \quad (2.18)$$

This result shows that the effective noise term is non-local in both space and time.

3 2PI effective action

We observed that the 1PI effective action is a convenient tool for deriving an equation of motion that takes into account long time tails in the evolution of the hydrodynamic field. This suggests that we can use higher nPI effective actions to derive similar equations of motion for higher n-point functions. In order to study 2PI and 3PI effective actions we will use a two-component notation $\psi_a = (\tilde{\psi}, \psi)$ for the hydrodynamic field. The quadratic action is

$$S = \frac{1}{2} \int d^3x dt \psi_a A_{ab} \psi_b, \quad (3.1)$$

with

$$A = \begin{pmatrix} 2\kappa T \nabla^2 & \partial_t - D \nabla^2 \\ -\partial_t - D \nabla^2 & 0 \end{pmatrix}. \quad (3.2)$$

In (ω, k) space this leads to the matrix propagator

$$G_{ab}^0 = \frac{1}{\omega^2 + (Dk^2)^2} \begin{pmatrix} 0 & -i\omega + Dk^2 \\ i\omega + Dk^2 & 2\kappa T k^2 \end{pmatrix}. \quad (3.3)$$

It is interesting to note that this propagator has the analytical structure of the Closed Time Path (CTP) propagator in the Keldysh basis, see, for example [37]. The interaction term can be written as

$$S = - \int d^3x dt \frac{\kappa \lambda_3}{2} c_{abc} (\nabla^2 \psi_a) \psi_b \psi_c, \quad (3.4)$$

with $c_{122} = 1$ and all others $c_{abc} = 0$. Note that other structures are also possible. As explained in [30] T -reversal invariance is consistent with a coupling of the form $c_{abc}\psi_a(\nabla\psi_b)(\nabla\psi_c)$ with $c_{211} = 1$ and all others $c_{abc} = 0$. In addition to the local source term in equ. (2.5) we also couple a bi-local source $\frac{1}{2}\psi_a K_{ab}\psi_b$. Then

$$\frac{\delta W}{\delta J_a} = \langle \psi_a \rangle = \Psi_a, \quad (3.5)$$

$$\frac{\delta W}{\delta K_{ab}} = \frac{1}{2} \langle \psi_a \psi_b \rangle = \frac{1}{2} [\Psi_a \Psi_b + G_{ab}], \quad (3.6)$$

where G_{ab} is the full two-point function. We can now perform a Legendre transform

$$\Gamma[\Psi_a, G_{ab}] = W[J_a, K_{ab}] - J_a \Psi_a - \frac{1}{2} K_{AB} [\Psi_A \Psi_B + G_{AB}], \quad (3.7)$$

where we have introduced the notation $F_A G_A = \int d^3x dt F_a G_a$. The 2PI effective action can be computed in analogy to 1PI action, using the background field method, see equ. (2.8). We obtain

$$\Gamma[\Psi_a, G_{ab}] = S[\Psi_a] + \frac{1}{2} \frac{\delta^2 S}{\delta \Psi_A \delta \Psi_B} G_{AB} - \frac{1}{2} \text{Tr} [\log(G)] + \Gamma_F[\Psi_a, G_{ab}], \quad (3.8)$$

where $G = \det G_{ab}$. The first term in equ. (3.8) is the classical action, and the third term is the one-loop correction generated by the full propagator G . The second term ensures that the leading term in the equation of motion for the propagator is $G = G^0$. Higher order fluctuations are described by Γ_F ,

$$\exp(-\Gamma_F[\Psi_a, G_{ab}]) = \frac{1}{\sqrt{\det(G)}} \int D(\delta\psi_a) \exp \left\{ -\frac{1}{2} \delta\psi_A (G^{-1})_{AB} \delta\psi_B - [S_3[\Psi_a, \delta\psi_a] - \bar{J}_A \delta\psi_A - \bar{K}_{AB} (\delta\psi_A \delta\psi_B - G_{AB})] \right\}, \quad (3.9)$$

where we have introduced [33]

$$\bar{J}_a = \frac{1}{2} \frac{\delta^3 S}{\delta \Psi_a \delta \Psi_B \delta \Psi_C} G_{BC} + \frac{\delta \Gamma_F}{\delta \Psi_a}, \quad \bar{K}_{ab} = \frac{\delta \Gamma_F}{\delta G_{ab}}. \quad (3.10)$$

We observe that Γ_F generates loop diagrams with the full propagator G_{ab} . The factor $\det(G)^{-1/2}$ removes the one-loop diagram already included in equ. (3.8). The action S_3 is defined in analogy with equ. (2.9)

$$S_3[\Psi_a, \delta\psi_a] = S[\Psi_a + \delta\psi_a] - \frac{\delta S}{\delta \Psi_a} \delta\psi_a - \frac{1}{2} \frac{\delta^2 S}{\delta \Psi_A \delta \Psi_B} \delta\psi_A \delta\psi_B. \quad (3.11)$$

Note that for a cubic interaction S_3 is not a function of the background field Ψ_a , and the only vertex in S_3 is that of the original action, given by equ. (3.4) with $\psi_a \rightarrow \delta\psi_a$. If we include a quartic interaction term, then S_3 contains a new vertex of the form

$$S_3[\Psi_a, \delta\psi_a] = \frac{\kappa \lambda_4}{3!} \int d^3x dt d_{abcd} [(\nabla^2 \Psi_a) \delta\psi_b \delta\psi_c \delta\psi_d + 3(\nabla^2 \delta\psi_a) \Psi_b \delta\psi_c \delta\psi_d], \quad (3.12)$$

$$\begin{pmatrix} \Sigma_{11} & \Sigma_{12} \\ \Sigma_{21} & \Sigma_{22} \end{pmatrix} = \begin{pmatrix} \text{Diagram 1} & \text{Diagram 2} \\ \text{Diagram 3} & \text{Diagram 4} \end{pmatrix}$$

Figure 4. Schwinger-Dyson equation for the self energies in the 2PI formalism.

where $d_{1222} = 1$ and all others $d_{abcd} = 0$. Finally, we note that the source terms in equ. (3.10) remove tadpoles order by order in the loop expansion of equ. (3.9).

The Legendre transform in equ. (3.7) is known as the 2PI effective action, because the loop expansion of equ. (3.9) corresponds to the sum of two-particle irreducible diagrams. The leading two-loop diagrams are shown in Fig. 3. These diagrams give

$$\begin{aligned} \Gamma_F[G_{ab}] = & \frac{1}{2} \left(\frac{\kappa\lambda_3}{2} \right)^2 \int d^3x dt d^3x' dt' \left\{ 2 \left(\nabla_x^2 \nabla_{x'}^2 G_{11}(x, t; x', t') \right) \left(G_{22}(x, t; x', t') \right)^2 \right. \\ & \left. + 4 \left(\nabla_x^2 G_{12}(x, t; x', t') \right) \left(\nabla_{x'}^2 G_{21}(x, t; x', t') \right) G_{22}(x, t; x', t') \right\}. \end{aligned} \quad (3.13)$$

Note that, as explained above, this result only depends on G_{ab} , and not on Ψ_a . We can now study the equation of motion that follows from equ. (3.8). We find

$$\Sigma_{ab} \equiv [G^{-1}]_{ab} - [G_0^{-1}]_{ab} = 2 \frac{\delta \Gamma_F[G]}{\delta G_{ab}}. \quad (3.14)$$

This is a self-consistent equation for the matrix self-energy Σ_{ab} . Note that in equ. (2.14,2.15) we denoted $\Sigma = \Sigma_{12}$ and $\delta D = \Sigma_{11}$. The equation of motion for Ψ_a is the same as in equ. (2.16), where Σ is given by the solution of equ. (3.14). For translationally invariant systems the consistency equation (3.14) is most easily stated in (ω, k) space. Using equ. (3.13) we get

$$\Sigma(\omega, k) \equiv \Sigma_{12}(\omega, k) = (\kappa\lambda_3)^2 \int d^3k' d\omega' (k+k')^2 k^2 G_{22}(\omega', k') G_{21}(\omega + \omega', k + k') \quad (3.15)$$

$$\delta D(\omega, k) \equiv \Sigma_{11}(\omega, k) = \frac{(\kappa\lambda_3)^2}{2} \int d^3k' d\omega' k^4 G_{22}(\omega', k') G_{22}(\omega + \omega', k + k'), \quad (3.16)$$

where G_{ab} is self-consistently determined by equ. (3.14). In components this relation is given in equ. (3.4,3.6) in reference [30]. For $G_{ab} = [G_0]_{ab}$ we get the perturbative result in equ. (2.14,2.15). Note that at the stationary point G_{11} and Σ_{22} vanish. This also implies that at the stationary point the 2-loop approximation to Γ_F in the cubic theory vanishes.

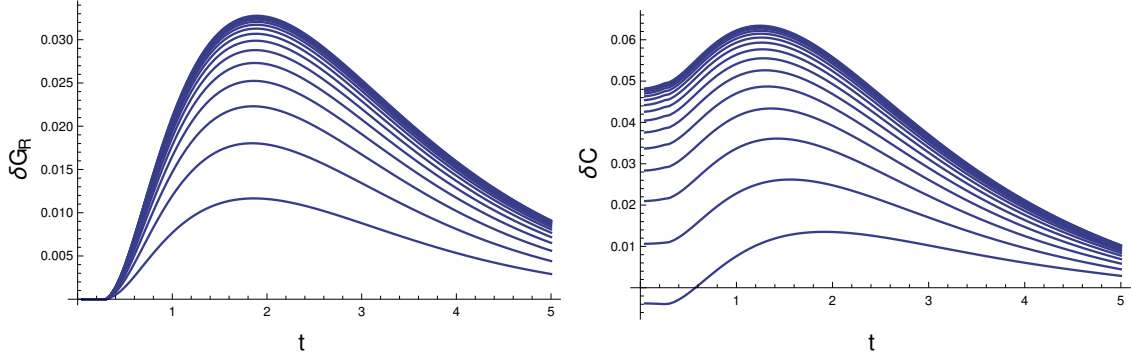


Figure 5. Loop corrections to the retarded Green function $\delta G_R(k, t) = G_R(k, t) - G_R^0(k, T)$ (left panel) and correlation function $\delta C(k, t) = C(k, t) - C^0(k, t)$ (right panel) as a function of t for fixed $k = 1$. We have also chosen $\lambda_3 = 2.5$ and $D = 1$. The different curves show the convergence of fixed-point iterations of the Schwinger-Dyson equation. The lowest curve is the result of the first iteration, corresponding to the one-loop result.

4 Gap equation in mixed representation

A practical approach to implementing equ. (3.15-3.16) is to solve the integral equations in a mixed representation $\Sigma_{ab}(t, k^2)$. In the mixed representation

$$\Sigma(t, k^2) = (\kappa\lambda_3)^2 \int d^3k' k^2 (k+k')^2 C(t, k') G_R(t, k+k'), \quad (4.1)$$

$$\delta D(t, k^2) = \frac{(\kappa\lambda_3)^2}{2} \int d^3k' k^4 C(t, k') C(t, k+k'). \quad (4.2)$$

In the mixed representation we need to solve the Dyson equation to close this set of equations. We have

$$G_{ab}(t, k^2) = G_{ab}^0(t, k^2) - \int dt_1 \int dt_2 G_{ac}^0(t_1, k^2) \Sigma_{cd}(t_2 - t_1, k^2) G_{db}(t - t_2, k^2). \quad (4.3)$$

The matrix product can be decomposed in terms of retarded, advanced, and symmetric functions. We find

$$\begin{aligned} G_R(t, k^2) &= G_R^0(t, k^2) - \int dt_1 \int dt_2 G_R^0(t_1, k^2) \Sigma_R(t_2 - t_1, k^2) G_R(t - t_2, k^2), \quad (4.4) \\ C(t, k^2) &= C^0(t, k^2) - \int dt_1 \int dt_2 \left[G_R^0(t_1, k^2) \delta D(t_2 - t_1) G_A(t - t_2, k^2) \right. \\ &\quad \left. + G_R^0(t_1, k^2) \Sigma_R(t_2 - t_1) C(t - t_2, k^2) \right. \\ &\quad \left. + C^0(t_1, k^2) \Sigma_A(t_2 - t_1) G_A(t - t_2, k^2) \right], \quad (4.5) \end{aligned}$$

where $C = G_{22}$, $G_R = G_{21}$, $G_A = G_{12}$ as well as $\Sigma_R \equiv \Sigma = \Sigma_{12}$, $\Sigma_A = \Sigma_{21}$, $\delta D = \Sigma_{11}$. The structure of equ. (4.4,4.5) ensures that the correlation functions have the correct symmetry, $G_R(t, k^2) = G_A(-t, k^2)$ and $C(t, k^2) = C(-t, k^2)$. The free propagator in the mixed representation given by

$$G_{ab}^0(t, k^2) = \begin{pmatrix} 0 & \Theta(-t) e^{Dtk^2} \\ \Theta(t) e^{-tDk^2} & \frac{T}{m^2} e^{-D|t|k^2} \end{pmatrix}. \quad (4.6)$$

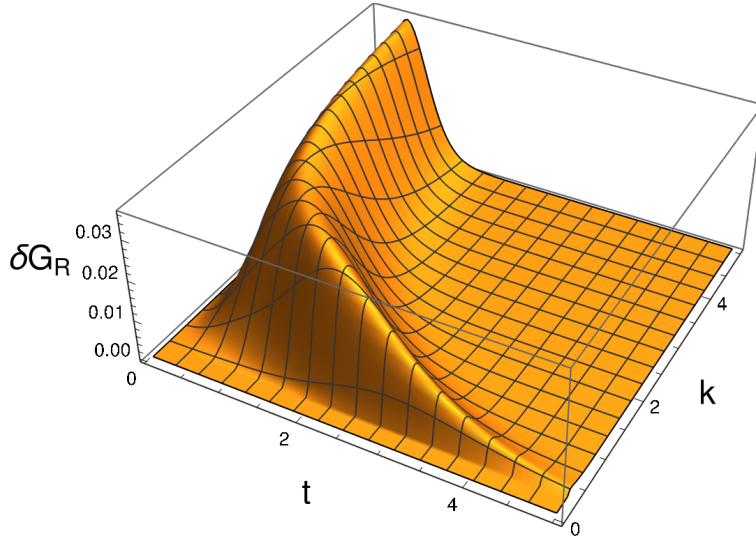


Figure 6. Loop corrections to the retarded Green function $\delta G_R(k, t)$ as a function of t and k . Parameters as in Fig. 5.

In the mixed representation, the gap equation (4.1,4.2) is UV finite, but there are short-time singularities in the Dyson equ. (4.3). This is clear from equ. (2.17), which shows that the one-loop self-energy contains terms of order $t^{-5/2}$ and $t^{-3/2}$. To regularize these singularities we have employed the Pauli-Villars method, see App. A. We add a number of hydrodynamic fields χ_i with diffusion constants $D_i \gg D$. These fields do not modify the Green functions for a large time, but the coupling constants can be adjusted to remove short-time singularities. Changing the D_i while adjusting the couplings to remove singularities in $\Sigma_{ab}(t, k^2)$ corresponds to adjusting polynomial terms in $\Sigma_{ab}(\omega, k^2)$.

A numerical solution of the Schwinger-Dyson equations (4.1,4.2) and (4.4,4.5) is shown in Figs. 5 and 6. We plot the loop corrections $\delta G_R = G_R - G_R^0$ and $\delta C = C - C^0$ to the retarded Green function and the correlation function. Note that the unit of length is given by the bare correlation length $\xi = m^{-1}$, and the unit of time is given by the relaxation time $\tau = \kappa/\xi^4$. The solutions are shown in dimensionless time units t and wave number k . Numerical solutions are obtained by iterating the gap equations (4.1,4.2) and the Dyson series (4.4,4.5) starting with the initial condition $G_{R,A} = G_{R,A}^0$ and $C = C^0$. This means that after one iteration we obtain the one-loop self-energy given in equ. (2.17).

The short time behavior is regularized with the help of two Pauli-Villars fields, see Appendix A. For the results shown in Figs. 5 and 6 we have used $(\alpha_{1,2}) = (4, 5)$, which means that the relaxation time of the Pauli-Villars diffusion is four and five times shorter, respectively, than that of the physical diffusion. There is a remaining $t^{-1/2}$ singularity, see App. A. This singularity is integrable, but in order to avoid numerical difficulties we also impose an explicit short-time cutoff $t_c = 0.2$. The results in Figs. 5 and 6 are obtained for $D = 1$ and $\lambda_3 = 2.5$.

We observe that the iterative solution of the Schwinger-Dyson equation is indeed con-

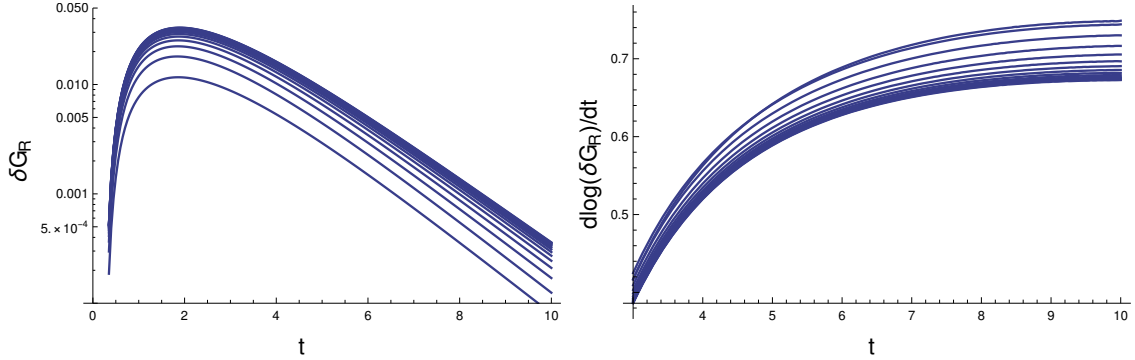


Figure 7. Long-time behavior of the loop corrections to the retarded Green function $\delta G_R(k, t)$. Parameters are chosen as in Fig. 5. The left panel shows a logarithmic plot of $\delta G_R(t, k^2)$ for $k = 1$ up to $t = 10$. The bottom curve is the one-loop result, and the top curve shows the converged solution of the Schwinger-Dyson equation. The right panel shows the logarithmic derivative of $\delta G_R(t, k^2)$ with respect to t . The top curve is the one-loop result, and the bottom one is the converged solution.

vergent. For small $\lambda_3 \sim 1$ the final solution is very close to the one-loop result. For larger values of λ_3 we observe significant corrections. In the regime $t \lesssim 1$ these deviations are very sensitive to the form of the regulator, but for $t \gtrsim 1$ the corrections are universal in the sense that changes in the regulator can be compensated by changes in the coupling. Loop corrections renormalize the strength of the coupling λ_3 . There is a critical value of the bare coupling beyond which no solutions of the Schwinger-Dyson can be found. The value of the critical coupling depends on the choice of the regulator. For the parameters used in Figures, $\alpha_{1,2} = (4.0, 5.0)$, the value of the critical coupling is $\lambda_{3,c} \simeq 2.58$. In Fig. 7 we analyze the long-time behavior of loop corrections to the retarded Green function in more detail. The left panel shows a logarithmic plot of $\delta G_R(t, k)$ up to larger times $t \leq 10$, and the right panel shows the logarithmic derivative of $\delta G_R(t, k^2)$ with respect to t . The one-loop correction decays as $\exp(-Dk^2t/2)$. Delacrétaz noticed that n -loop terms scale as $n! \exp(-Dk^2t/n)$, and conjectured that the long-time behavior of the diffusion cascade is $\exp(-\alpha\sqrt{DK^2t})$ with $\alpha \sim 1$ [38]. Our results are consistent with the emergence of a cascade – we observe that the logarithmic derivative of δG_R decreases as higher and higher loops are summed – but it is difficult to establish the behavior at asymptotically long times.

5 Conclusions and Outlook

In this work we have studied the 1PI and 2PI effective actions for the stochastic diffusion equation. We have numerically investigated solutions of the Schwinger-Dyson equation derived from the 2-loop 2PI action in a model with a cubic coupling. We find that higher loop corrections summed by the Schwinger-Dyson equation renormalize the coupling constant, and we observe indications of a diffusion cascade at long times.

This existence of the diffusion cascade implies that the long-time behavior of diffusion is non-perturbative, even in a non-critical fluid. We can estimate the relevant

time scale based on equ. (2.17). For this purpose we use $m = \xi^{-1}$ and $\kappa = \xi^4/\tau$, where ξ is the correlation length and τ is the relaxation time. We also write the non-linear coupling as $\lambda_3 = g_3/(\xi^{3/2}T^{1/2})$, where g_3 is dimensionless. The one-loop correction $\delta G_R \sim \exp(-Dk^2t/2)$ decays more slowly than the tree level term $G_R^0 = \exp(-Dk^2t)$. The two terms are comparable if

$$t \gtrsim \frac{2\tau}{(k\xi)^2} \log \left(\frac{2}{\alpha g_3^2 (k\xi)^2} \right), \quad (5.1)$$

where $\alpha = 1/(64\sqrt{2}\pi^{3/2})$ is the numerical constant in equ. (2.17). For $g_3 = O(1)$ fluctuations with wave number $k = \xi^{-1}$ are non-perturbative for $t \gtrsim 2\tau \log(2/\alpha) \sim 12\tau$. In the case of a relativistic heavy ion collision we have previously used the estimate $\xi \simeq 1.2$ fm and $\tau = 1.8$ fm [12, 39]. This means that non-perturbative effects set in for $t \gtrsim 20$ fm, too large to be relevant in a heavy ion collision in which the life time of the fireball is on the order of 10 fm. Modes with $k > \xi^{-1}$ become non-perturbative earlier, but in that case higher order hydrodynamic effects are also important.

The methods described in this work can be extended in a variety of ways. One direction is to compute the 3PI effective action, and determine the self-consistent equation for the three-particle vertex. Note that the third Legendre transform, even though it is usually referred to as the 3PI effective action, is not the sum of all 3PI diagrams. Indeed, in a theory with only a cubic interaction there are no 3PI diagrams, but one can nevertheless construct an effective action that generates a self-consistent vertex function [40, 41].

Another interesting direction is to consider the critical regime, both for a purely diffusive theory and for a theory of a conserved density coupled to the momentum density of the fluid. These theories are known as model B and model H in the classification of Hohenberg and Halperin [13]. Model H describes the critical endpoint in a single component fluid, and is also believed to describe a possible endpoint of the quark-gluon plasma transition in QCD [42]. There are several approaches for extracting the critical correlation functions. The first is the ϵ -expansion, in which physical quantities are computed as an expansion around the critical dimension. A second approach, known as mode coupling theory [43], is based on approximate solutions of self-consistent equations. The nPI method provides a way to systematically check these approximations and extend the results to higher n -point functions. A related approach is the functional renormalization group (FRG), which has also been applied to critical dynamics [44]. An advantage of functional methods such as the FRG or the nPI method is that they can serve as a starting point for deriving approximate kinetic equations. These kinetic equations may provide a practical approach to critical dynamics in systems, such as heavy ion collisions, in which there is a non-trivial background flow.

Acknowledgments

This work is supported by the U.S. Department of Energy Office of Nuclear Physics through Contract DE-FG02-03ER41260 (T.S.). The work of J.C. is supported by start-up funding from Jiangxi Normal University under grant No. 12021211. T.S. would like to thank Alexander Kemper for useful discussions, and Luca Delacrétaz for pointing us to [38].

A Pauli-Villars Regulator

We consider the effective lagrangian for a diffusive field ψ in the presence of Pauli-Villars regulator fields χ_i ($i = 1, \dots, N_{PV}$),

$$\mathcal{L} = \tilde{\psi} \left(\partial_t \psi - \kappa \nabla^2 \frac{\delta \mathcal{F}}{\delta \psi} \right) + \tilde{\psi} \kappa T \nabla^2 \tilde{\psi} + \tilde{\chi}_i \left(Z_{ij}^{-1} \partial_t \chi_j - \bar{\kappa}_{ij} \nabla^2 \frac{\delta \mathcal{F}}{\delta \chi_j} \right) + \tilde{\chi}_i \bar{\kappa}_{ij} T \nabla^2 \tilde{\chi}_j, \quad (\text{A.1})$$

with

$$\mathcal{F} = \int d^3x \left\{ \frac{1}{2} (\nabla \psi)^2 + \frac{1}{2} m^2 \psi^2 + \frac{\lambda_3}{3!} \psi^3 + \frac{1}{2} (\nabla \chi_i)^2 + \frac{1}{2} \bar{m}_{ij}^2 \psi_i \psi_j + \frac{\bar{\lambda}_{ij}}{2} \psi \chi_i \chi_j \right\}. \quad (\text{A.2})$$

In the following we will assume that $Z_{ij} = \delta_{ij}$. The lagrangian in equ. (A.1) is of the form

$$\mathcal{L} = \tilde{s}_a (\partial_t s_a - V(s)) + \tilde{s}_a \kappa_{ab} \tilde{s}_b, \quad V_a(s) = -\kappa_{ab} \frac{\delta \mathcal{F}}{\delta s_b}, \quad (\text{A.3})$$

where κ_{ab} is a symmetric matrix and $s_a = (\psi, \chi_i)$ as well as $\tilde{s}_a = (\tilde{\psi}, \tilde{\chi}_i)$. This lagrangian has a time reversal invariance

$$\mathcal{T} s_a(t) \rightarrow s_a(-t), \quad (\text{A.4})$$

$$\mathcal{T} \tilde{s}_a(t) \rightarrow \left[-\tilde{s}_a(-t) + \frac{\delta \mathcal{F}}{\delta s_a} \right]. \quad (\text{A.5})$$

under which $\mathcal{L} \rightarrow \mathcal{L} + (d\mathcal{F})/(dt)$. The time reversal symmetry ensures that detailed balance and fluctuation-dissipation relations are satisfied in the presence of the regulator fields.

We will also take the matrices \bar{m}_{ij} , $\bar{\kappa}_{ij}$ and $\bar{\lambda}_{ij}$ to be diagonal, and denote $\bar{m}_{ij} = \delta_{ij} \bar{m}_i$ etc. The quadratic part of the lagrangian is

$$\mathcal{L} = \tilde{\psi} (\partial_t - \kappa m^2 \nabla^2) \psi + \tilde{\psi} \kappa T \nabla^2 \tilde{\psi} + \tilde{\chi}_i (\partial_t - \bar{\kappa}_i^2 \bar{m}_i^2 \nabla^2) \chi_i + \tilde{\chi}_i \bar{\kappa}_i T \nabla^2 \tilde{\chi}_i. \quad (\text{A.6})$$

We allow the $(\tilde{\chi}_i, \chi_i)$ to be ghost fields, so that loops acquire an extra minus sign. We also define $\bar{\kappa}_i = \alpha_i \bar{\kappa}$ and set $\bar{m}_i^2 = m^2$. This implies that the diffusion constant of the Pauli-Villars fields is

$$\bar{D}_i = \alpha_i D. \quad (\text{A.7})$$

The non-linear interaction terms are

$$\mathcal{L} = -\frac{\kappa \lambda_3}{2} (\nabla^2 \tilde{\psi}) \psi^2 - \frac{\kappa \bar{\lambda}_i}{2} (\nabla^2 \tilde{\psi}) \chi_i \chi_i - \bar{\kappa} \bar{\lambda}_i (\nabla^2 \tilde{\chi}_i) \psi \chi_i, \quad (\text{A.8})$$

and we define

$$\bar{\lambda}_i^2 = c_i \lambda_3^2. \quad (\text{A.9})$$

The Pauli-Villars fields are then characterized by the parameters (α_i, c_i) . We will adjust these parameters to remove the UV divergences in the self energy.

Consider the one-loop contribution to the retarded self energy $\Sigma(t, k^2)$, see equ. (2.17). In the presence of Pauli-Villars fields the leading short time behavior is

$$\Sigma(t, k^2) = \frac{3}{64\sqrt{2}\pi^{3/2}} \frac{\lambda_3^2 T}{m^6 \sqrt{D}} \left\{ \frac{1}{t^{5/2}} \left[1 + \sum \frac{c_i}{\alpha_i^{1/2}} \right] - \frac{Dk^2}{6t^{3/2}} \left[1 + \sum_i c_i \alpha_i^{1/2} \right] + O\left(\frac{1}{t^{1/2}}\right) \right\}. \quad (\text{A.10})$$

The terms of order $t^{-5/2}$ and $t^{-3/2}$ lead to divergences in the Fourier transform $\Sigma(\omega, k^2)$ and the convolution integral in the Dyson equation, see equ. (4.3). If we define a short-time cutoff $t_c \sim (D\Lambda^2)^{-1}$ then $\int dt/t^{5/2} \sim \Lambda^3$ and $\int dt/t^{3/2} \sim \Lambda$. We can eliminate these divergences by choosing suitable Pauli-Villars fields. These have to satisfy

$$1 + \sum \frac{c_i}{\alpha_i^{1/2}} = 0, \quad 1 + \sum_i c_i \alpha_i^{1/2} = 0. \quad (\text{A.11})$$

The minimal number of fields is two. In this case we have

$$c_1 = \alpha_1^{1/2} \frac{\alpha_2 - 1}{\alpha_1 - \alpha_2}, \quad c_2 = -\alpha_2^{1/2} \frac{\alpha_1 - 1}{\alpha_1 - \alpha_2}. \quad (\text{A.12})$$

We can choose any set of $\alpha_{1,2} > 1$ as long as $\alpha_1 \neq \alpha_2$. Different choices of these parameters correspond to different values of higher order transport coefficients. We note that one of the c_i is negative, corresponding to a ghost field. A consistency check is provided by computing $\delta D(t, k^2)$. Once the (α_i, c_i) are fixed by the requirement that short-time singularities in $\Sigma(t, k^2)$ are removed, then $\delta D(t, k^2)$ should be non-singular as well. This is indeed the case.

References

- [1] Misha A. Stephanov, K. Rajagopal, and Edward V. Shuryak. Signatures of the tricritical point in QCD. *Phys. Rev. Lett.*, 81:4816–4819, 1998.
- [2] Adam Bzdak, Shinichi Esumi, Volker Koch, Jinfeng Liao, Mikhail Stephanov, and Nu Xu. Mapping the Phases of Quantum Chromodynamics with Beam Energy Scan. *Phys. Rept.*, 853:1–87, 2020.
- [3] Marcus Bluhm et al. Dynamics of critical fluctuations: Theory – phenomenology – heavy-ion collisions. *Nucl. Phys. A*, 1003:122016, 2020.
- [4] Xin An et al. The BEST framework for the search for the QCD critical point and the chiral magnetic effect. *Nucl. Phys. A*, 1017:122343, 2022.
- [5] S. Ejiri, F. Karsch, and K. Redlich. Hadronic fluctuations at the QCD phase transition. *Phys. Lett. B*, 633:275–282, 2006.
- [6] M. A. Stephanov. Non-Gaussian fluctuations near the QCD critical point. *Phys. Rev. Lett.*, 102:032301, 2009.
- [7] Masayuki Asakawa, Shinji Ejiri, and Masakiyo Kitazawa. Third moments of conserved charges as probes of QCD phase structure. *Phys. Rev. Lett.*, 103:262301, 2009.
- [8] M. A. Stephanov. On the sign of kurtosis near the QCD critical point. *Phys. Rev. Lett.*, 107:052301, 2011.
- [9] B. Friman, F. Karsch, K. Redlich, and V. Skokov. Fluctuations as probe of the QCD phase transition and freeze-out in heavy ion collisions at LHC and RHIC. *Eur. Phys. J. C*, 71:1694, 2011.
- [10] Boris Berdnikov and Krishna Rajagopal. Slowing out-of-equilibrium near the QCD critical point. *Phys. Rev. D*, 61:105017, 2000.
- [11] Marlene Nahrgang, Marcus Bluhm, Thomas Schäfer, and Steffen A. Bass. Diffusive dynamics of critical fluctuations near the QCD critical point. *Phys. Rev. D*, 99(11):116015, 2019.

- [12] Yukinao Akamatsu, Derek Teaney, Fanglida Yan, and Yi Yin. Transits of the QCD critical point. *Phys. Rev. C*, 100(4):044901, 2019.
- [13] P. C. Hohenberg and B. I. Halperin. Theory of Dynamic Critical Phenomena. *Rev. Mod. Phys.*, 49:435–479, 1977.
- [14] R. Folk and Hans-Guenther Moser. Critical dynamics: a field-theoretical approach. *J. Phys. A*, 39:R207–R313, 2006.
- [15] Jurgen Berges, Soren Schlichting, and Denes Sexty. Dynamic critical phenomena from spectral functions on the lattice. *Nucl. Phys. B*, 832:228–240, 2010.
- [16] Dominik Schweitzer, Sören Schlichting, and Lorenz von Smekal. Spectral functions and dynamic critical behavior of relativistic Z_2 theories. *Nucl. Phys. B*, 960:115165, 2020.
- [17] Dominik Schweitzer, Sören Schlichting, and Lorenz von Smekal. Critical dynamics of relativistic diffusion. *Nucl. Phys. B*, 984:115944, 2022.
- [18] Grégoire Pihan, Marcus Bluhm, Masakiyo Kitazawa, Taklit Sami, and Marlene Nahrgang. Critical net-baryon fluctuations in an expanding system. *Phys. Rev. C*, 107(1):014908, 2023.
- [19] Thomas Schäfer and Vladimir Skokov. Dynamics of non-Gaussian fluctuations in model A. *Phys. Rev. D*, 106(1):014006, 2022.
- [20] Chandrodoy Chattopadhyay, Josh Ott, Thomas Schaefer, and Vladimir Skokov. Dynamic scaling of order parameter fluctuations in model B. 4 2023.
- [21] Swagato Mukherjee, Raju Venugopalan, and Yi Yin. Real time evolution of non-Gaussian cumulants in the QCD critical regime. *Phys. Rev. C*, 92(3):034912, 2015.
- [22] Yukinao Akamatsu, Aleksas Mazeliauskas, and Derek Teaney. A kinetic regime of hydrodynamic fluctuations and long time tails for a Bjorken expansion. *Phys. Rev. C*, 95(1):014909, 2017.
- [23] M. Stephanov and Y. Yin. Hydrodynamics with parametric slowing down and fluctuations near the critical point. *Phys. Rev. D*, 98(3):036006, 2018.
- [24] M. Martinez and Thomas Schäfer. Stochastic hydrodynamics and long time tails of an expanding conformal charged fluid. *Phys. Rev. C*, 99(5):054902, 2019.
- [25] Xin An, Gökçe Başar, Mikhail Stephanov, and Ho-Ung Yee. Relativistic Hydrodynamic Fluctuations. *Phys. Rev. C*, 100(2):024910, 2019.
- [26] Xin An, Gökçe Başar, Mikhail Stephanov, and Ho-Ung Yee. Fluctuation dynamics in a relativistic fluid with a critical point. *Phys. Rev. C*, 102(3):034901, 2020.
- [27] Xin An, Gökçe Başar, Mikhail Stephanov, and Ho-Ung Yee. Evolution of Non-Gaussian Hydrodynamic Fluctuations. *Phys. Rev. Lett.*, 127(7):072301, 2021.
- [28] Hong Liu and Paolo Glorioso. Lectures on non-equilibrium effective field theories and fluctuating hydrodynamics. *PoS*, TASI2017:008, 2018.
- [29] Xinyi Chen-Lin, Luca V. Delacrétaz, and Sean A. Hartnoll. Theory of diffusive fluctuations. *Phys. Rev. Lett.*, 122(9):091602, 2019.
- [30] Jingyi Chao and Thomas Schäfer. Multiplicative noise and the diffusion of conserved densities. *JHEP*, 01:071, 2021.
- [31] Noriyuki Sogabe and Yi Yin. Off-equilibrium non-Gaussian fluctuations near the QCD critical point: an effective field theory perspective. *JHEP*, 03:124, 2022.

- [32] Juergen Berges. Introduction to nonequilibrium quantum field theory. *AIP Conf. Proc.*, 739 (1):3–62, 2004.
- [33] Esteban A. Calzetta and Bei-Lok B. Hu. *Nonequilibrium Quantum Field Theory*. Cambridge Monographs on Mathematical Physics. Cambridge University Press, 11 2022.
- [34] P.C. Martin, E.D. Siggia, and H.A. Rose. Statistical Dynamics of Classical Systems. *Phys. Rev. A*, 8:423–437, 1973.
- [35] Hans-Karl Janssen. On a lagrangean for classical field dynamics and renormalization group calculations of dynamical critical properties. *Zeitschrift für Physik B*, 23:377–380, 1976.
- [36] C. De Dominicis and L. Peliti. Field Theory Renormalization and Critical Dynamics Above $t(c)$: Helium, Antiferromagnets and Liquid Gas Systems. *Phys. Rev. B*, 18:353–376, 1978.
- [37] Alex Kamenev and Alex Levchenko. Keldysh technique and nonlinear sigma-model: Basic principles and applications. *Adv. Phys.*, 58:197, 2009.
- [38] Luca V. Delacrétaz. Heavy Operators and Hydrodynamic Tails. *SciPost Phys.*, 9(3):034, 2020.
- [39] M. Martinez, T. Schäfer, and V. Skokov. Critical behavior of the bulk viscosity in QCD. *Phys. Rev. D*, 100(7):074017, 2019.
- [40] Cyrano de Dominicis and Paul C. Martin. Stationary Entropy Principle and Renormalization in Normal and Superfluid Systems. I. Algebraic Formulation. *J. Math. Phys.*, 5:14–30, 1964.
- [41] Cyrano de Dominicis and Paul C. Martin. Stationary Entropy Principle and Renormalization in Normal and Superfluid Systems. II. Diagrammatic Formulation. *J. Math. Phys.*, 5:31–59, 1964.
- [42] D. T. Son and M. A. Stephanov. Dynamic universality class of the QCD critical point. *Phys. Rev. D*, 70:056001, 2004.
- [43] K. Kawasaki. Kinetic equations and time correlation functions of critical fluctuations. *Ann. Phys.*, 61:1, 1970.
- [44] Léonie Canet and Hugues Chaté. A non-perturbative approach to critical dynamics. *J. Phys. A*, 40(9):1937–1949, 2007.